Inorganic Chemistry Research
Article

Effect of Transition Metals on the Structural, Electrical and Optical Properties of Fullerene C_{20}

Elham Hedayatirad[a], Pouran Pourhakkak[b,*], Hadis Mohammadpour[a], Hamidreza Shamlouei[a] and Zohreh Khajehali[a]

[a]*Chemistry Department, Lorestan University, Khorram Abad*
[b]*Department of Chemistry, Payame Noor University, P.O. Box 19395-1697, Tehran, Iran*

Received: August 30, 2021; Accepted: November 8, 2021
Cite This: *Inorg. Chem. Res.* **2021**, *5*, 252-256. DOI: 10.22036/icr.2021.294424.1111

Abstract: In the present study, the effect of transition elements on structural properties and electronic and linear optical and nonlinear optical (NLO) properties of fullerene C_{20} was studied by replacing the transitions elements such as Sc, Ti, V, Cr, Mn, Fe, Co, Ni, Cu, Zn with one of the C_{20} carbon atoms at theoretical B3LYP/6-31+G(d) level. Frequency calculations for all optimized structures show no imaginary frequency which is the important evidence for their stability. It was observed as the result of the doping of transition metals the values of E_g (highest occupied molecular orbital–lowest unoccupied molecular orbital gap) was reduced which shows improving the electrical properties of the C_{20} by doping the transition metal atoms instead of one of the carbon atom. Additionally, transition metal doping in the C_{20} nanocluster enhances its dipole moment which the $C_{19}Sc$ nanocluster has the highest and the $C_{19}Cu$ has the lowest dipole moment. Finally, it has been demonstrated that in the presence of the first raw transition metal of periodic table in C_{20}, the values of polarizability and first hyperpolarizability (α and β_0) increases which the highest values of α and β_0 was obtained *via* Sc and Mn atoms doping.

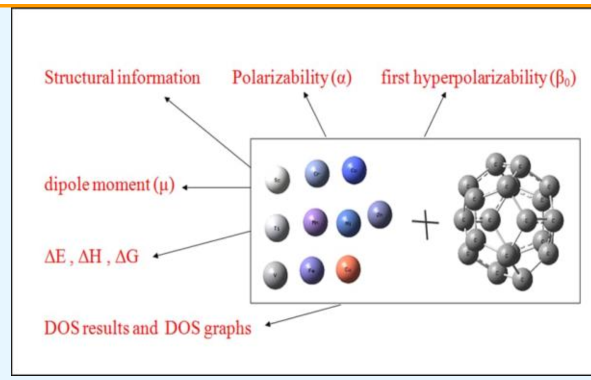

Keywords: Fullerene C_{20}, Nonlinear optical property (NLO), Transition metals, Density functional theory (DFT), The first hyperpolarizability (β_0)

1. INTRODUCTION

After the discovery of carbon nanotubes by Ajima, which made a huge revolution in the science and technology of nanomaterials, scientists showed a tendency to discover new materials with little dimensions.[1] Recently, nanoscale structures have been discovered in the form of fullerene cages with the general formula, C_n (n = 20, 22, 24, 30, 60, ...). It has been shown that these homologues of fullerene molecules have excellent applications in electronic devices, imaging materials, magnetic recording, and environmental processes; so, their investigation will be very interesting.[2,3] By doping the transition metals into fullerenes structure, some of the properties of this structure are being changed significantly. When the first applied laser was discovered in the 1960s, linear optical properties were not shown, which is why nonlinear optics (NLO) appeared.[4] Regarding difference between linear and nonlinear optics, it can be declared that, in linear optics, a momentary polarization of the electron density of an atom is produced under the influence of an electromagnetic field, and there is a nonlinear relation between the non-induction polarization and the field. But in nonlinear optics, the material responds to a large-size field and the material's response to the field is nonlinear. Non-linear optics is related to light behavior in nonlinear materials, which is commonly observed at high light intensities such as the intensity of pulsed lasers.[5] Conventionally, lithium niobite ($LiNbO_3$) and potassium dihydrogen phosphate (KDP) are molecules that have significant nonlinear optics. Theoretical calculations of linear and nonlinear properties (NLO) are highly remarked by semi-experimental methods, because the information about the material with higher NLO, can show how the synthesis strategy can be.[6-10] Normally, there are linear and nonlinear properties (NLO) in materials with existence containing polar molecules with no symmetrical center arrangement, such as polarized polymers or crystals lacking a symmetry center.[11-23] Some effort was done to improve the NLO properties of nanomaterials such as doping the alkali metal atoms on the surface of nanomaterials[24,25], doping the transition metal on nanoclusters,[26,27] and decorating nanoclusters with superalkali metal oxides M3O.[28-30] In this work,

$C_{19}M$ (M = Sc, Ti, V, Cr, Mn, Fe, Co, Ni, Cu, Zn) nanoclusters are constructed by doping the first raw transition metals in the periodic table into fullerene C_{20} cells. Moreover, the linear and nonlinear optical (NLO) and electrical properties, as well as geometric parameters such as bond length and bond angles and their energy, are studied.

2. COMPUTATIONAL METHOD

The $C_{19}M$ (M = Sc, Ti, V, Cr, Mn, Fe, Co, Ni, Cu, Zn) nanoclusters were completely optimized at theoretical B3LYP/6-31+G(d) level.[32,33] Frequency calculations of all optimized structures were done at the same level. For calculation of the properties of odd metal atoms doping, the unrestricted method was used. Density of States (DOS) was calculated with GaussSum.3.3.9 program.[34] The HOMO–LUMO (highest occupied molecular orbital–lowest unoccupied molecular orbital) gap (E_g) values of structures were achieved from the difference between ε_H (HOMO energy) and ε_L (LUMO energy). Polarizability (α) and the first hyperpolarizability (β_0) properties were examined respectively, as linear optical and non-linear optical (NLO) at the theoretical CAM-B3LYP/6-31+G(d) level. The first hyperpolarizability (β_0) is a factor for NLO response coefficient. It was calculated by using the following equations:

$$\beta_0 = (\beta_x^2 + \beta_y^2 + \beta_z^2)^{\frac{1}{2}} \qquad (1)$$

and

$$\beta_i = \frac{3}{5}(\beta_{iii} + \beta_{ijj} + \beta_{ikk}) \quad i, j, k = X, Y, Z \qquad (2)$$

Also, ΔE, ΔH and ΔG were calculated by using the following equations:

$$\Delta E = [E(C_{19}X) + E(C)] - [E(C_{20}) + E(X)] \qquad (3)$$

$$\Delta H = [H(C_{19}X)+H(C)] - [H(C_{20}) + H(X)] \qquad (4)$$

$$\Delta G = [G(C_{19}X) + G(C)] - [G(C_{20}) + G(X)] \qquad (5$$

All calculations were accomplished with Gaussian 09 package.[35]

3. RESULTS AND DISCUSSION

For better understanding of the content, the optimized structures studied are shown in Figure 1.

In the structures shown in Figure 1, three types of bond lengths can be identified. Using the structures and bond lengths, it has been attempted to observe the effects of doping the transition metal atoms on the C_{20} structure. The angle between the carbon-metal-carbon was also measured. The corresponding numerical data obtained are summarized in Table 1.

As seen in Table 1, the length of the metal bond with the cluster is different in these compounds. The highest metal bond with carbon in the case of a scandium is equal to 2.11 Å with the bond angle of C-M-C (M is transition metal atom) equals to 81.95. The shortest link length is also seen in the doping of the C_{20} cluster with the chromium atom. The reported values for the transition metal atoms radius are presented in Table 2.

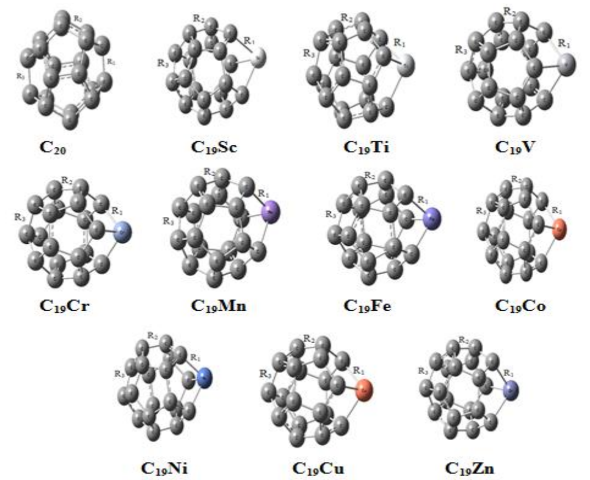

Figure 1. Optimized structures of $C_{19}M$ nanoclusters.

Table 1. Structural information on the length bonds and angles of the C_{20} and $C_{19}M$ nanoclusters

Structure	R_1 (Å)	R_2 (Å)	R_3 (Å)	C-X-C (Degree)
C_{20}	1.44	1.48	1.44	-
$C_{19}Sc$	2.11	1.45	1.46	81.95
$C_{19}Ti$	1.95	1.44	1.46	94.41
$C_{19}V$	1.98	1.45	1.46	84.82
$C_{19}Cr$	1.85	1.46	1.45	86.85
$C_{19}Mn$	1.90	1.46	1.48	87.25
$C_{19}Fe$	1.89	1.47	1.45	81.54
$C_{19}Co$	1.91	1.46	1.45	85.52
$C_{19}Ni$	1.89	1.46	1.46	94.15
$C_{19}Cu$	2.00	1.46	1.45	86.07
$C_{19}Zn$	2.02	1.46	1.45	85.53

Table 2. The atomic radii of 1st row transition metal atoms

Sc	164	Ti	147	V	135
Cr	129	Mn	137	Fe	126
Co	125	Ni	125	Cu	128
Zn	137	.			

Various parameters act on the M-C bond length and so no distinct relations were found between the values of atomic radii and M-C bond length. The value of R3 for the $C_{19}Mn$ is higher than the calculated values of other nanoclusters which may be the result of d^5 electronic configuration in Mn atom.

The density of the electronic states or the DOS spectrum for all considered nanoclusters was then plotted. These DOS diagrams are shown in Figures 2 and 3 for $C_{19}Sc$, $C_{19}Ti$, $C_{19}V$, $C_{19}Cr$, $C_{19}Mn$, $C_{19}Fe$, $C_{19}Co$, $C_{19}Ni$, $C_{19}Cu$, $C_{19}Zn$ nanoclusters with HOMO and LUMO orbital maps for each of them.

The energy of HOMO and LUMO was calculated using the electron state density spectra for different nanoclusters. Using these energies, the distance of the gap was also calculated. In Table 2, the energy values of HOMO, LUMO and the gap are collected.

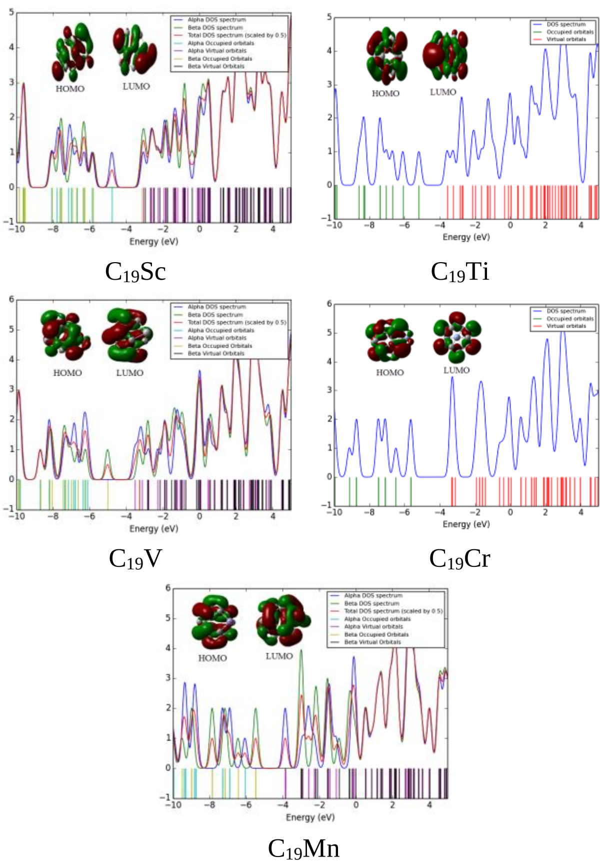

Figure 2. DOS spectra and HOMO, LUMO profiles of $C_{19}M$ (M = Sc, Ti, V, Cr, Mn).

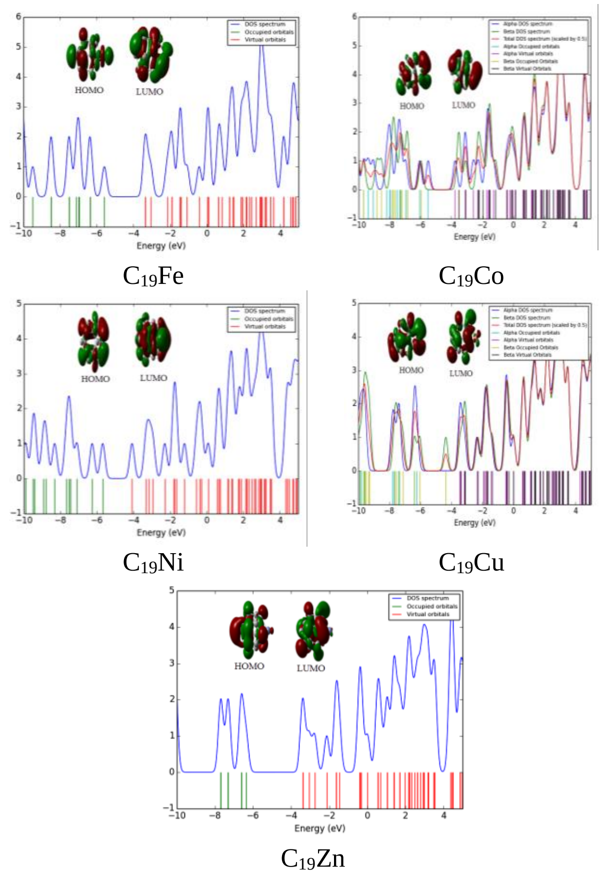

Figure 3. DOS spectra and HOMO, LUMO profiles of $C_{19}M$ (M = Fe, Co, Ni, Cu, Zn).

As the result, it was shown that the E_g for most of the nanoclusters reduced. However, in some cases, these E_g values increased. The value of $\%\Delta E_g$ shows the percent of the relative difference of E_g in comparison to pristine C_{20} fullerene and can be defined as;

$$\Delta E_g = \frac{E_g(C_{19}M) - E_g(C_{20})}{E_g(C_{20})} \times 100$$

In the case of reduction of E_g as the result of transition metal doping, the value of $\%\Delta E_g$ is negative. In HOMO-LUMO gap no electronic states exist. So the intensity of DOS shows the number of electronic states in each energy. It seems that the number of electrons in d orbitals may be the factor of difference between the nanoclusters.

Results of calculation the energy, enthalpy and free energy calculation for doping the transition metal on C20 nanocluster are listed in Table 3. As seen, all ΔE, ΔH and ΔG values are positive, therefore their preparation with direct reaction is impossible. It is clear for the preparation of these nanoclusters, the row material with higher content of energy must be used.

Table 2. the values of E_{HOMO}, E_{LUMO}, E_g and $\%\Delta E_g$ for the C_{20} and $C_{19}M$ nanoclusters

Structure	E_H (eV)	E_L (eV)	E_g (eV)	ΔE_g (%)
C_{20}	-5.5	-3.62	1.88	-
$C_{19}Sc$	-4.78	-3.13	1.65	-12.23
$C_{19}Ti$	-5.19	-3.59	1.6	-14.89
$C_{19}V$	-5.02	-3.53	1.49	-20.74
$C_{19}Cr$	-5.65	-3.33	2.32	23.40
$C_{19}Mn$	-5.48	-3.86	1.62	-13.83
$C_{19}Fe$	-5.59	-3.35	2.24	19.15
$C_{19}Co$	-5.51	-3.76	1.75	-6.915
$C_{19}Ni$	-5.69	-4.09	1.6	-14.89
$C_{19}Cu$	-6.04	-4.36	1.68	-10.63
$C_{19}Zn$	-6.36	-3.39	2.97	57.98

The dipole momentum of the fullerene C_{20} is zero. By doping the transition metals, the dipole moment increases. The highest dipole moment increase is 3.5 which belongs to the $C_{19}Sc$ nanocluster. The results in Table 4 show that doping of metals leads to an increase in dipole moments and the regular C_{20} fullerene has the lowest dipole moment.

The amount of polarizability in the C_{20} is 188.17. Doping of transition metals increases the amount of polarizability. Among these nanoclusters, the highest polarizability value belongs to the $C_{19}Sc$. So, it indicates that molecules containing metal have more polarizability. Also, the metal doping process increased the value of the first hyperpolarizability for all nanoclusters. In the nanoclusters, the highest value of the first hyperpolarizability (β_0) belongs to the $C_{19}Mn$ nanocluster.

Table 3. ΔE, ΔH and ΔG values of $C_{19}M$ nanoclusters

Structure	ΔE (kcal mol^{-1})	ΔH (kcal mol^{-1})	ΔG (kcal mol^{-1})
$C_{19}Sc$	99.56	95.66	96.03
$C_{19}Ti$	69.69	66.11	66.25
$C_{19}V$	67.40	63.69	64.30
$C_{19}Cr$	76.64	72.44	73.41
$C_{19}Mn$	81.00	77.04	77.89
$C_{19}Fe$	66.11	63.57	64.88
$C_{19}Co$	130.51	127.39	128.05
$C_{19}Ni$	113.95	122.11	111.44
$C_{19}Cu$	174.44	170.93	171.02
$C_{19}Zn$	193.32	190.54	191.61

Table 4. Polarizability (α), the first hyperpolarizability (β_0) and dipole moment (μ) values of $C_{19}M$ nanoclusters

Structure	β_0 (a.u.)	α (a.u.)	μ (a.u)
C_{20}	0.3975	188.17	0.00
$C_{19}Sc$	2232.55	223.02	3.50
$C_{19}Ti$	1528.42	217.04	2.58
$C_{19}V$	1871.64	219.47	2.20
$C_{19}Cr$	890.79	212.30	1.59
$C_{19}Mn$	5400.46	213.82	1.31
$C_{19}Fe$	1767.24	207.95	1.58
$C_{19}Co$	1279.45	208.98	1.26
$C_{19}Ni$	832.52	206.41	0.85
$C_{19}Cu$	634.36	206.69	0.84
$C_{19}Zn$	642.41	205.91	1.18

4. CONCLUSION

In the present study, the quantum-mechanics calculation of the effects of doping transition metals on electrical properties and linear and nonlinear optical properties (NLO) of fullerene C_{20} was investigated. The results of the calculations indicated that the doping of transition metals was reduced regarding the distance between the highest occupied molecular orbitals (HOMO) and the lowest unoccupied molecular orbitals (LUMO) in the $C_{19}M$ nanoclusters. The electrical properties of the molecule were improved by doping the metal on C_{20}. Also, satisfactory results in terms of nonlinear optics in the structures were observed, so that the dipole moment, the polarizability and the first hyperpolarizability increases. According to the DOS graphs, the least energy of the gap is found for vanadium doping and the greatest energy of gap was due to the doping of the zinc metal in fullerene. The results of the dipole moment indicate that the doping of transition metals on the C_{20} increases dipole moment. The $C_{19}Sc$ nanocluster has the highest and the $C_{19}Cu$ has the lowest dipole moment. By comparing dipole moments of nanoclusters with fullerene C_{20} (with zero the dipole moment), it can be concluded that all nanoclusters are more polarized than fullerene C_{20}. In general, it has been proved in the present study that the presence of the first raw transition metal of periodic table in C_{20}, increases μ, α and β_0, and somewhat decreases in E_g and bond lengths compared to non-metallic molecules. Also, the value of C_{20} fullerene doping with Sc and Mn increases the values of μ, α and β_0.

CONFLICTS OF INTEREST

There are no conflicts to declare.

AUTHOR INFORMATION

Corresponding Author(s)

Pouran Pourhakkak: Email: p_pourhakkak@pnu.ac.ir

Author(s)

Elham Hedayatirad, Hadis Mohammadpour, Hamidreza Shamlouei, Zohreh Khajehali

REFERENCES

1. S. Iijima, *Nature*, **1991**, *354*, 56-58.
2. V. Talyzin, I. Engström, *J. Phys. Chem. B*, **1998**, *102*, 34, 6477-6481.
3. R. C. Haddon, A. F. Hebard, M. J. Rosseinsky, D. W. Murphy, S. J. Duclos, K. B. Lyons, B. Miller, J. M. Rosamilia, R. M. Fleming, A. R. Kortan, S. H. Glarum, A. V. Makhija, A. J. Muller, R. H. Eick, S. M. Zahurak, R. Tycko, G. Dabbagh, F. A. Thiel, *Nature*, **1991**, *350*, 320-322.
4. T. H. Maiman, *Nature*, **1960**, *187*, 493.
5. P. A. Franken, A. E. Hill, C. W. Peters, G. Werinreich, *Phys. Rev. Lett.* **1961**, *7*, 118.
6. D. A. Kleinman, *Phys. Rev*., **1962**, *126*, 1977-1979.
7. D. R. Kanis, M. A. Ratner, T.J. Marks, *Chem. Rev*., **1994**, *94*, 195-242.
8. V. J. Docherty, D. Pugh, J. O. Morley, *J. Chem. Soc*., *Faraday Trans*. **1985** *2*, *81*, 1179-1192.
9. Ulman, *J. Chem*., **1988**, *92*, 2385-90.
10. D. R. Kanis, M. A. Ratner, T. J. Marks, M. C. Zerner, *Chem. Mater*., **1991**, *3*, 19.
11. D. M. Burland, R. D. Miller, C. A. Walsh, *Chem. Rev*., **1994**, *94*, 31-75.
12. G. R. Meredith, J. G. VanDusen, D. J. Williams, *Macromolecules*, **1982**, *15*, 1385.
13. E. Kelderman, G. J. T. Heesink, L. Derhaeg, T. Verbiest, P. T. A. Klaase, W. Verboom, J. F. J. Engbersen, N. F. van Hulst, K. Clays, A. Persoons, D. N. Reinhoudt. *Adv. Mater*., **1993**, *5*, 925.
14. J. Wu, J. Valley, S. Ermer, E. Binkley, J. Kenney, G. Lipscomb, R. Lytel, *Appl. Phys. Lett*., **1991**, *58*, 225.
15. Teraoka, D. Jungbauer, B. Reck, D. Yoon, R. Twieg, C. Willson, *J. Appl. Phys*., **1991**, *69*, 2568.
16. D. Dai, M. Hubbard, J. Park, T. J. Marks, J. Wang, G. K. Wong, *Mol. Cryst. Liq. Cryst*., **1990**, *189*, 93.
17. Xu, B. Wu, L. R. Dalton, P. M. Ramon, Y. Shi, W. H. Steier, *Macromolecules*, **1992**, *25*, 4032.
18. K. M. White, C. V. Francis, A. J. Isackson, *Macromolecules*, **1994**, *27*, 3519-24.
19. Y. Haruvy, S. Webber, *Chem. Mater*., **1991**, *3*, 501.

20. G. Puccetti, E. Toussaere, I. Ledoux, J. Zyss, *Polym. Prepr*., ***1991***, *32*, 61.
21. E. Toussaere, J. Zyss, P. Griesmar, C. Sanchez, *Nonlinear Opt*., **1991**, *1*, 349.
22. R. J. Jeng, Y. M. Chen, A. K. Jain, J. Kumar, S. K. Tripathy, *Chem. Mater*., **1992**, *4*, 972.
23. J. Zyss, J. F. Nicoud, M. Coquillay, *J. Chem. Phys*., **1984**, *81*, 4160.
24. E. Shakerzdeh , E. Tahmasebi, H. R. Shamlouei, *Synthetic Metals*, **2015**, *204* , 17-24.
25.F. Tahmaszadeh, H. R. Shamloue, *Int. J. Nanoelectron. Mater*., **2018**, *11*, 1-14.
25. H. R. Shamlouei, A. Nouri, A. Mohammadi, A. Dadkhah Tehrani, *Physica E*, **2016**, *77*, 48-53.
26.M. Omidi, H. R. Shamlouei, M. Noormohammadbeigi, *J. Mol. Model*, **2017**, *23,* 82.
27. M. Noormohammadbeigi1, H. R. Shamlouei, *J. Inorg. Organomet. Polym*., **2018**, *28*, 110-120.
28. R. Toosi1, H. R. Shamloue, A. Mohammadi Hesari, *Chinese Phys. B*, **2016**, *25*, 094220.
29. M. Omidi, M. Sabzehzarib H. R. Shamlouei, *Chinese J. Phys*., **2020**, *65*, 567-578.
30. D. Becke, *J. Chem. Phys*., **1993**, *98*. 5648.
31. Lee, W. Yang, R. G. Parr, *Phys. Rev. B*, **1988**, *37*, 785.
32. N. M. O'boyle, A. L. Tenderholt, K. M. Langner, *J. Comp. Chem*., **2008**, *29*, 839.
33. M. J. Frisch, G. W. Trucks, H. B. Schlegel, G. E. Scuseria, M. A. Robb, J. R. Cheeseman, G. Scalmani, V. Barone, B. Mennucci, G. A. Petersson, H. Nakatsuji, M. Caricato, X. Li, H. P. Hratchian, A. F. Izmaylov, J. Bloino, G. Zheng, J. L. Sonnenberg, M. Hada, M. Ehara, K. Toyota, R. Fukuda, J. Hasegawa, M. Ishida, T. Nakajima, Y. Honda, O. Kitao, H. Nakai, T. Vreven, J. A. Montgomery, Jr., J. E. Peralta, F. Ogliaro, M. Bearpark, J. J. Heyd, E. Brothers, K. N. Kudin, V. N. Staroverov, R. Kobayashi, J. Normand, K. Raghavachari, A. Rendell, J. C. Burant, S. S. Iyengar, J. Tomasi, M. Cossi, N. Rega, J. M. Millam, M. Klene, J. E. Knox, J. B. Cross, V. Bakken, C. Adamo, J. Jaramillo, R. Gomperts, R. E. Stratmann, O. Yazyev, A. J. Austin, R. Cammi, C. Pomelli, J. W. 34. Ochterski, R. L. Martin, K. Morokuma, V. G. Zakrzewski, G. A. Voth, P. Salvador, J. J. Dannenberg, S. Dapprich, A. D. Daniels, Ö. Farkas, J. B. Foresman, J. V. Ortiz, J. Cioslowski, and D. J. Fox, Gaussian 09 (Gaussian, Inc., Wallingford CT), **2009**.